


Cite this: *RSC Adv.*, 2021, **11**, 288

## Synthetic and thermal studies of four insensitive energetic materials based on oxidation of the melamine structure†

Jiarong Zhang, <sup>a,c</sup> Fuqiang Bi, <sup>\*bc</sup> Junlin Zhang, <sup>c</sup> Xiaohong Wang, <sup>c</sup> Zhi Yang, <sup>a</sup> Guofang Zhang<sup>b</sup> and Bozhou Wang <sup>\*c</sup>

Oxidation of nitrogen-rich aromatic heterocycles has a significant impact on the development of energetic materials. 2,4,6-Triamino-1,3,5-triazine-1,3-dioxide (MDO) is a promising insensitive energetic backbone obtained from melamine under strong oxidation conditions with impressive thermal behaviors and detonation performances. In this paper, MDO was prepared with improved yields of 85% and its thermal behavior, non-isothermal decomposition kinetics and gas products were investigated in detail. The corresponding decomposition mechanism was also deduced by applying the TG-DSC-FTIR-MS technique for the first time. The decomposition temperature of MDO reaches 300 °C and the apparent activation energy of MDO (*E*) calculated by the Kissinger and Ozawa method proved to be 303.63 and 279.95 kJ mol<sup>-1</sup>, indicating great thermal stability. Three new monoanionic energetic salts with impressively improved properties were achieved based on the basicity of MDO with yields of >80%. Their thermal decomposition temperatures proved to be higher than 230 °C and their densities are in the range of 1.75–1.89 g cm<sup>-3</sup>. The calculations and experiments show that their detonation velocities (*V<sub>D</sub>*: 8711–9085 m s<sup>-1</sup>) are comparable to or exceed those of RDX (*D*: 8795 m s<sup>-1</sup>) while the sensitivities to impact (IS: 23–27 J) and friction (FS: >240 J) are much lower.

Received 25th October 2020  
Accepted 28th November 2020

DOI: 10.1039/d0ra09105g  
rsc.li/rsc-advances

### Introduction

The introduction of *N*-oxide moieties can greatly improve the physical properties and detonation performances of energetic materials.<sup>1–10</sup> During the past few decades, *N*-oxide rich aromatic heterocycles have attracted intensive attention and numerous novel *N*-oxide rich energetic structures, such as 1,2,3,4-tetrazino[5,6-*e*]-1,2,3,4-tetrazine-1,3,6,8-tetraoxide (TTTO),<sup>11,12</sup> 1-hydroxy-1*H*-[1,2,3]triazolo[4,5-*e*] [1,2,3,4]tetrazine 5,7-dioxide (HTTDO),<sup>13,14</sup> and [1,2,5] oxadiazolo [3,4-*e*] [1,2,3,4] tetrazine 4,6-di-*N*-oxide<sup>15</sup> were successfully achieved. From a structural point of view, strong hydrogen bonds will be formed by incorporating nitro or *N*-oxide groups with adjacent amino groups and typical structures include 2,6-diamino-3,5-dinitropyrazine-1-oxide (LLM-105),<sup>16,17</sup> triamino-5-dinitropyrimidine-1,3-dioxide (ICM-102),<sup>18</sup> and 3,8-

dinitropyrazolo[5,1-*c*][1,2,4] triazine-4,7-diamine.<sup>19</sup> However, the preparations of these energetic structures still suffer multistep synthesis and a simple synthetic method is highly needed.<sup>20</sup>

Unlike nitro groups, *N*-oxide moieties are embedded in the molecular backbones and therefore, lead to more compact packings. Melamine is a trimer of cyanamide with a 1,3,5-triazine skeleton and has been extensively used for chemical engineering. Selective oxidation of melamine (Scheme 1) will be a straightforward strategy for the synthesis of hydrogen bond rich structure. For instance, 2,4,6-triamino-1,3,5-triazine-1,3-dioxide (MDO)<sup>21,22</sup> is a promising insensitive heat-resistant energetic compounds in weaponry with high decomposition temperature (*T<sub>d</sub>*: >300 °C) and low impact sensitivity (IS: >20 J). In this paper, we synthesized the MDO by H<sub>2</sub>O<sub>2</sub>/CF<sub>3</sub>COOH oxidation with improved yield, moreover, by tuning with energetic anion (ClO<sub>4</sub><sup>-</sup>, N(NO<sub>2</sub>)<sub>2</sub><sup>-</sup> and NO<sub>3</sub><sup>-</sup>), three new insensitive energetic monoanionic salts, including perchlorate salt of MDO (MDOP), dinitramide salt (MDONA) and mono nitrate salt (MDOMN) with significantly improved properties were prepared based on the basicity of MDO *via* ion exchange reaction. A comprehensively study of their thermal behaviors, non-isothermal decomposition kinetics and the thermal decomposition mechanisms were also carried out for the first time by using TG-DSC-FTIR-MS technique. In addition, the densities and sensitivities (to impact, friction and electrostatic-spark)

<sup>a</sup>School of Chemistry and Chemical Engineering, Beijing Institute of Technology, Beijing, 100081, PR China

<sup>b</sup>Key Laboratory of Applied Surface and Colloid Chemistry, MOE/School of Chemistry and Chemical Engineering, Shaanxi Normal University, Xi'an 710062, PR China. E-mail: bifuqiang@gmail.com

<sup>c</sup>State Key Laboratory of Fluorine & Nitrogen Chemicals, Xi'an Modern Chemistry Research Institute, Xi'an 710065, PR China. E-mail: wbz600@163.com

† Electronic supplementary information (ESI) available. CCDC 1947761. For ESI and crystallographic data in CIF or other electronic format see DOI: 10.1039/d0ra09105g



were investigated by experimental approaches and the detonation performances were calculated.

## Experiment

**General caution!** Although we have experienced no explosion accident in synthesis and characterization of these materials, proper protective measures should be adopted.

### Materials and instruments

Ammonium perchlorate, ammonium dinitramide and ammonium nitrate were supplied by Xi'an Modern Chemistry Research Institute. Melamine, trifluoroacetic acid and hydrogen peroxide aqueous used in the study were purchased and used directly without further purification. The dehydrated MDO sample was used for the DSC-TG-MS-FTIR, density and sensitivity tests.  $^1\text{H}$  NMR and  $^{13}\text{C}$  NMR spectra were obtained on a Bruker 500 MHz spectrometer in deuterated dimethyl sulfoxide at room temperature, using trimethyl silane (TMS) as internal standard. The infrared spectra were recorded on a Nicolet NEXUS870 infrared spectrometer in the range of  $4000\text{ cm}^{-1}$  to  $400\text{ cm}^{-1}$  in KBr matrix. Elemental analysis (C, H and N) were carried out on a VARI-E1-3 elementary analysis instrument. The DSC and TG studies were undertaken on a TGA/DSC Mettler Toledo calorimeter at a heating rate of  $10\text{ }^\circ\text{C min}^{-1}$ , under dry oxygen-free nitrogen atmosphere with a flowing rate of  $50\text{ mL min}^{-1}$ . The impact and friction sensitivities were determined using the BAM method. Electrostatic-spark sensitivities ( $E_{50}$ ) were measured on HT-201B-3 electrostatic-spark sensitivity tester, under electrode gap of 0.5 mm, electric capacity of 10 000 pF,  $E_{50} = 1/2CV(50)^2$ . The synchronous thermal analysis was undertaken on a Germany Benz 449C TG-DSC synchronous thermal analyzer. The operation conditions are as follows: sample mass is about 0.35 mg, the crucible is made of aluminum, heating rates are 2.5, 5.0, 10.0 and  $20.0\text{ }^\circ\text{C min}^{-1}$ , the flow rate of the dynamic argon gas atmosphere is  $25\text{ mL min}^{-1}$ . Infrared spectrometer was carried out on American Nicolet 5700 infrared spectrometer in the range of  $4000\text{--}650\text{ cm}^{-1}$ . The operation conditions are as follows: the detector is DTGS; resolution  $> 0.09\text{ cm}^{-1}$ ; purge gas flow is  $50\text{ mL min}^{-1}$ ; protective gas flow is  $25\text{ mL min}^{-1}$ . The operating temperature of MS connection tube (sampling capillary) is  $190\text{ }^\circ\text{C}$ . Mass spectrometer was made on a Germany NETZSCH QMS403 quadrupole mass spectrometer. The operation conditions are as follows: the temperature of thermal analysis instrument and mass spectrometry and interface is  $200\text{ }^\circ\text{C}$ ; the test mass range is between 1–300 amu; the resolution is  $< 0.5\text{ amu}$  and the detection limit  $> 1\text{ ppm}$ .



Scheme 1 Selective oxidation of melamine.

### Synthetic procedures

#### Synthesis of 2,4,6-triamino-1,3,5-triazine-1,3-dioxide (MDO).

Melamine (0.5 g, 4 mmol) was suspended in 12 mL trifluoroacetic acid at  $0\text{ }^\circ\text{C}$ , then 5 mL 50% hydrogen peroxide aqueous was slowly added. After maintaining at room temperature for 5 h, white precipitate was filtered and dissolved in water. Then, the solution was neutralized to  $\text{pH} = 7$  with  $\text{NaHCO}_3$ , colorless precipitate was filtered out, washed with a small amount of cold water, and dried as 2,4,6-triamino-1,3,5-triazine-1,3-dioxide tetrahydrate (MDO· $4\text{H}_2\text{O}$ ) (0.78 g, 85% yield).  $^1\text{H}$  NMR (500 MHz,  $\text{DMSO}-d_6$ ):  $\delta$  ppm: 9.33 (s, 2H,  $\text{NH}_2$ ), 8.80 (s, 4H,  $\text{NH}_2$ );  $^{13}\text{C}$  NMR (125 MHz,  $\text{DMSO}-d_6$ ):  $\delta$  ppm: 150.97, 152.76; IR  $\nu$ : 3416, 3346, 3185, 1678, 1467, 1428, 1250, 1196, 1140, 827, 798, 720, 680, 607  $\text{cm}^{-1}$ ; elemental analysis calculated (%) for MDO· $4\text{H}_2\text{O}$ : C 15.65, H 6.13, N 36.51; found: C 15.37, H 6.04, N 37.21. MDO· $4\text{H}_2\text{O}$  (2 g) was putted in a round bottom flask and heated to  $130\text{ }^\circ\text{C}$  for 1 h to obtain MDO without  $\text{H}_2\text{O}$  (1.35 g). Elemental analysis calculated (%) for MDO: C 22.79, H 3.82, N 53.15; found: C 23.01, H 3.75, N 53.35.

#### Synthesis of perchlorate salt of 2,4,6-triamino-1,3,5-triazine-1,3-dioxide (MDOP).

Melamine (0.5 g, 4 mmol) was suspended in 12 mL trifluoroacetic acid at  $0\text{ }^\circ\text{C}$ , then 5 mL hydrogen peroxide aqueous (50%) was slowly added. After maintaining at room temperature for 5 h, white precipitate was filtered and dissolved in water. Ammonium perchlorate (0.41 g, 3.5 mmol) was added in batches, and the reaction was carried out at  $0\text{ }^\circ\text{C}$  for 1 h, white precipitate was filtered and the filter cake was washed with cold water, drying in the air to get MDOP (0.83 g, 81% yield).  $^1\text{H}$  NMR (500 MHz,  $\text{DMSO}-d_6$ ):  $\delta$  ppm: 8.69 (s, 2H,  $\text{NH}_2$ ), 9.14 (s, 2H,  $\text{NH}_2$ ), 9.37 (s, 2H,  $\text{NH}_2$ );  $^{13}\text{C}$  NMR (125 MHz,  $\text{DMSO}-d_6$ ):  $\delta$  ppm: 151.92, 152.63; IR  $\nu$ : 3427, 3360, 3290, 1682, 1661, 1506, 1254, 1113, 1084, 728, 628  $\text{cm}^{-1}$ ; elemental analysis calculated (%) for MDOP: C 13.94, H 2.73, N 32.50; found: C 13.72, H 2.87, N 32.64.

#### Synthesis of dinitramide salt of 2,4,6-triamino-1,3,5-triazine-1,3-dioxide (MDONA).

Melamine (0.5 g, 4 mmol) was suspended in 12 mL trifluoroacetic acid at  $0\text{ }^\circ\text{C}$ , then 5 mL hydrogen peroxide aqueous (50%) was slowly added. After maintaining at room temperature for 5 h, white precipitate was filtered and dissolved in water. Ammonium dinitramide (0.44 g, 3.5 mmol) was added in batches, and the reaction was carried out at  $0\text{ }^\circ\text{C}$  for 1 h, white precipitate was filtered and the filter cake was washed with cold water, drying in the air to get MDONA (0.87 g, 83% yield).  $^1\text{H}$  NMR (500 MHz,  $\text{DMSO}-d_6$ ):  $\delta$  ppm: 8.69 (s, 2H,  $\text{NH}_2$ ), 9.14 (s, 2H,  $\text{NH}_2$ ), 9.37 (s, 2H,  $\text{NH}_2$ );  $^{13}\text{C}$  NMR (125 MHz,  $\text{DMSO}-d_6$ ):  $\delta$  ppm: 151.92, 152.63; IR  $\nu$ : 3416, 3278, 3134, 1674, 1648, 1510, 1437, 1327, 1244, 1171, 1010, 894  $\text{cm}^{-1}$ ; elemental analysis calculated (%) for MDONA: C 13.59, H 2.66, N 47.54; found: C 13.41, H 2.82, N 47.60.

#### Synthesis of mono nitrate salt of 2,4,6-triamino-1,3,5-triazine-1,3-dioxide (MDOMN).

Melamine (0.5 g, 4 mmol) was suspended in 12 mL trifluoroacetic acid at  $0\text{ }^\circ\text{C}$ , then 5 mL hydrogen peroxide aqueous was slowly added. After maintaining at room temperature for 5 h, white precipitate was filtered and dissolved in water. Ammonium nitrate (0.28 g, 3.5 mmol) was added in batches, and the reaction was carried out at  $0\text{ }^\circ\text{C}$



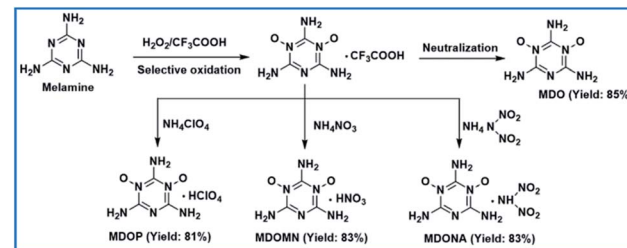
for 1 h, white precipitate was filtered and the filter cake was washed with cold water, drying in the air to get  $\text{MDOMN}\cdot\text{H}_2\text{O}$  (0.73 g, 83% yield).  $^1\text{H}$  NMR (500 MHz,  $\text{DMSO}-d_6$ ):  $\delta$  ppm: 8.72 (s, 2H,  $\text{NH}_2$ ), 9.14 (s, 2H,  $\text{NH}_2$ ), 9.39 (s, 2H,  $\text{NH}_2$ );  $^{13}\text{C}$  NMR (125 MHz,  $\text{DMSO}-d_6$ ):  $\delta$  ppm: 151.92, 152.62; IR  $\nu$ : 3597, 3433, 3165, 1668, 1644, 1499, 1384, 1316, 1246, 1185, 892, 726, 665  $\text{cm}^{-1}$ ; elemental analysis calculated (%) for  $\text{MDOMN}\cdot\text{H}_2\text{O}$ : C 15.07, H 3.79, N 41.00; found: C 15.19, H 3.75, N 41.93.

## Results and discussion

### Controllable synthesis

In the melamine molecule, both the amino group and the N atom on the triazine backbone are reaction sites that could be oxidized, so which site is more reactive? We conducted comparative analyses of the reactivities of melamine and 1,3,5-triazine molecules through the surface electrostatic potential (ESP). It was found that the introduction of the three amino groups to the triazine backbone structure (Fig. 1a) completely changes the charge distribution of the 1,3,5-triazine (Fig. 1b). In the melamine molecule, the electron cloud distribution is concentrated on the triazine backbone and the N atom due to the p- $\pi$  conjugation effect between the amino groups and the triazine ring, so that the triazine ring and the nitrogen atom are both negatively charged. The surface minimum point of melamine is located on the N atoms of triazine backbone with value of  $-30.27$  kcal  $\text{mol}^{-1}$ . Moreover, due to the electron-withdrawing effect of the N atoms on the H atoms in the amino groups, the H atoms exhibit positive charge with the surface maximum point value of  $32.98$  kcal  $\text{mol}^{-1}$ . Therefore, in the melamine molecular structure, the N atoms on the triazine ring are easier to be oxidized than the amino groups.

Initially, we commenced our experiments using  $\text{H}_2\text{O}_2/\text{HCOOH}$  and  $\text{H}_2\text{O}_2/\text{CH}_3\text{COOH}$  as oxidant and melamine as starting material (Scheme 3). Unfortunately, we didn't obtain MDO at the temperatures of  $20^\circ\text{C}$ ,  $40^\circ\text{C}$  or  $60^\circ\text{C}$ , and mixture products were generated, possibly caused by the weak oxidation



Scheme 3 The synthesis of MDO, MDOP, MDONA and MDOMN.

capacity of the chosen oxidants that leads to poor selectivity. Subsequently, we employed 50%  $\text{H}_2\text{O}_2/\text{CF}_3\text{COOH}$  and 98%  $\text{H}_2\text{O}_2/\text{CF}_3\text{COOH}$  as the oxidants respectively, and two nitrogen atoms of melamine were oxidized successfully, generating MDO with improved yield of 85%. While the yield of MDO was only around 50% when 30%  $\text{H}_2\text{O}_2/\text{CF}_3\text{COOH}$  was used as the oxidant due to the weakening of the oxidation capacity.<sup>22</sup> Both elemental analysis and single-crystal X-ray diffraction indicated that the MDO existed as tetrahydrate, and  $\text{H}_2\text{O}$  molecules could be completely removed by heating  $\text{MDO}\cdot 4\text{H}_2\text{O}$  sample at  $130^\circ\text{C}$ . It is noteworthy that using the cheap and readily available melamine as starting material and this one-step synthetic strategy with simple post-treatment, the large-scale production of MDO could potentially be achieved.

MDO is a nitrogen-rich energetic compound. It is readily to be protonated to generate MDO ionic salts, taking advantage of the negative polarity of oxygen atoms or nitrogen atoms. Siwei Song *et al.*<sup>22</sup> reported two dianionic salts of MDO (2,4,6-triamino-1,3,5-triazine-1,3-dioxide- $\text{HNO}_3$  (TTDON) and 2,4,6-triamino-1,3,5-triazine-1,3-dioxide- $\text{HClO}_4$  (TTDOP)) prepared *via* three-step reactions with the yields of 40% and 54% under strong acid solutions. However, the impact sensitivities of these two compounds are 14 J and 13 J, respectively, which is dangerous for further synthesis and storage of them (Scheme 2).

Here, using intermediate  $\text{MDO}\cdot\text{CF}_3\text{COOH}$  as starting material, three new MDO energetic monoanionic salts were prepared by ion exchange reaction, with yields ranging from 81% to 87%. Compared with TTDON and TTDOP, the strategy applied in our paper exhibits shorter reaction time, higher yields and safer operations.

### Thermal analysis of MDO

Thermal analysis is important for the production, storage, transportation, and application of energetic materials. The thermal behavior, non-isothermal decomposition kinetics and gas products generated from thermal decomposition of MDO were investigated in detail by using a set of specific experimental devices (*i.e.*, TG-DSC-FTIR-MS technique), under the heating rate of 2.5, 5, 10 and  $20^\circ\text{C min}^{-1}$ . Based on the results, the thermal decomposition mechanism of MDO was deduced. Fig. 2 shows the DSC-TG trace of MDO under a heating rate of  $10^\circ\text{C min}^{-1}$ . MDO commenced to decompose around  $273.4^\circ\text{C}$  without melting process. With the increasing of temperature, the decomposition of MDO became more intense, reaching the maximum at around  $318.9^\circ\text{C}$ . It is noteworthy that the

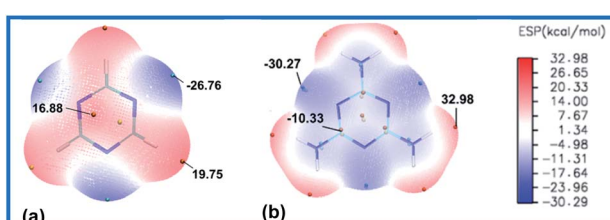
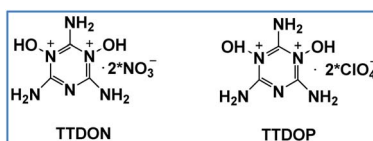


Fig. 1 (a) Electrostatic potential of 1,3,5-triazine; (b) electrostatic potential of melamine.



Scheme 2 The structures of TTDON and TTDOP.<sup>22</sup>



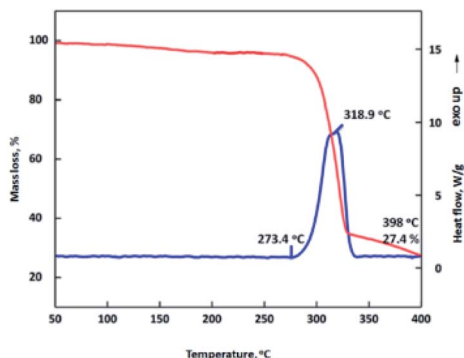
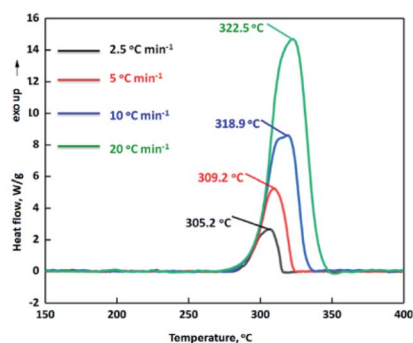
Fig. 2 DSC-TG trace of MDO under a heating rate of  $10\text{ }^{\circ}\text{C min}^{-1}$ .

Fig. 3 DSC traces of MDO at different heating rates.

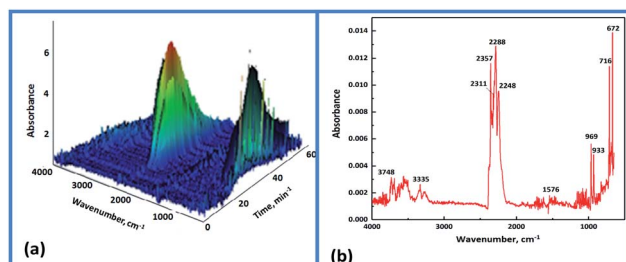
decomposition temperature of MDO is comparable to that of the reference thermostable HNS explosive ( $T_d$ :  $315\text{ }^{\circ}\text{C}$ ), indicating MDO possess a good thermal stability.

In order to get further information about the thermal decomposition process of MDO, the reaction kinetic parameters during the heating process of MDO were studied by Kissinger's and Ozawa-Doyle's method.<sup>23-25</sup> The DSC traces at different heating rates ( $2.5, 5, 10$  and  $20\text{ }^{\circ}\text{C min}^{-1}$ ) were shown in Fig. 3. The apparent activation energy  $E$  for the thermal decomposition of MDO calculated by Kissinger and Ozawa method is  $303.63\text{ kJ mol}^{-1}$  and  $279.95\text{ kJ mol}^{-1}$ , respectively (Table 1). Notably, the linear correlation coefficients ( $r$ ) calculated by Kissinger's method (0.9903) and Ozawa's method (0.9896) are very close and greater than 0.98. So the calculated results are

Table 1 Kinetic parameters and enthalpies of thermal decomposition of MDO

$\beta$ $\text{K min}^{-1}$	$T_p\text{ K}$	$E^a/\text{kJ mol}^{-1}$		$r^b$		$\ln(A_k^c\text{ s}^{-1})$
		Kissinger	Ozawa	Kissinger	Ozawa	
2.5	542.32	303.63	279.95	0.9903	0.9896	91.44
5	546.33					
10	556.09					
20	559.65					

<sup>a</sup> Apparent activation energy. <sup>b</sup> Liner correlation coefficient. <sup>c</sup> Pre-exponential factor.

Fig. 4 (a) 3D IR absorption spectrum of MDO at a heating rate of  $10\text{ }^{\circ}\text{C min}^{-1}$ ; (b) IR spectrum of MDO at  $319\text{ }^{\circ}\text{C}$ .

credible and provide a good reference for the thermal safety of MDO.

FTIR and MS are used for *in situ* tracking analysis, providing a comprehensive profile of the gas products. The three-dimensional IR absorption spectrum of MDO is shown in Fig. 4a, illustrating the changes of absorbance intensity of gases released during the decomposition of MDO with time (temperature) under a heating rate of  $10\text{ }^{\circ}\text{C min}^{-1}$ . The gas products started to appear about  $270\text{ }^{\circ}\text{C}$ , and the concentration reached maximum at around  $319\text{ }^{\circ}\text{C}$ . The changing trend of absorbance intensity is in good consistency with DSC-TG curve (Fig. 2). From the infrared spectrum of the gas generated at  $319\text{ }^{\circ}\text{C}$  (Fig. 4b), the gas products are identified as:  $\text{H}_2\text{O}$  ( $3748, 1576\text{ cm}^{-1}$ ),  $\text{CO}_2$  ( $2357, 2311, 2288, 672\text{ cm}^{-1}$ ),  $\text{N}_2\text{O}$  ( $2248\text{ cm}^{-1}$ ),  $\text{HCN}$  ( $716\text{ cm cm}^{-1}$ ),  $\text{NH}_3$  ( $3335, 969, 933\text{ cm}^{-1}$ ).

The mass spectrum of the gas products generated during thermal decomposition of MDO (Fig. 5) indicates the relationship between MS ion current intensity and temperature. The intensity of MS ion current originated from each gas fragment reaches highest at around  $319\text{ }^{\circ}\text{C}$ , which is in good consistency with DSC characterization (Fig. 2) and three-dimensional IR analysis (Fig. 4a). These results also suggest that MDO decomposed directly and intensely around this temperature. From the mass of the ion fragments, the gas products generated from thermal decomposition of MDO are assigned to:  $\text{NH}_3$  ( $m/z = 15, 16, 17$ ),  $\text{NO}$  ( $m/z = 30$ ),  $\text{NO}_2$  ( $m/z = 46$ ),  $\text{N}_2\text{O}$  or  $\text{CO}_2$  ( $m/z = 44$ ),  $\text{H}_2\text{O}$  ( $m/z = 18$ ),  $\text{CO}$  or  $\text{N}_2$  ( $m/z = 28$ ),  $\text{HN}=\text{C}=\text{NH}$  ( $m/z = 42$ ),  $\text{HCN}$  ( $m/z = 26, 27$ ). Since  $\text{N}_2$  is infrared inactive and  $\text{CO}$  was not

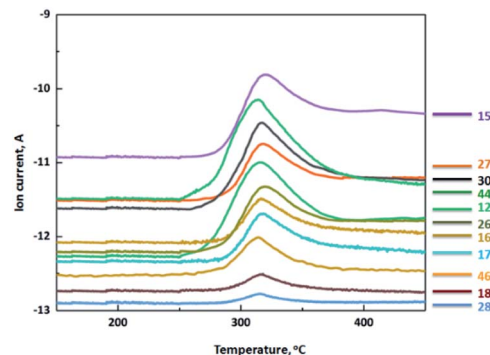
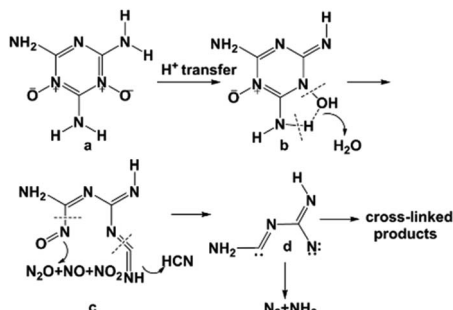


Fig. 5 The mass spectra of the gas products generated from thermal decomposition of MDO.



Scheme 4 Plausible thermal decomposition mechanism of MDO.

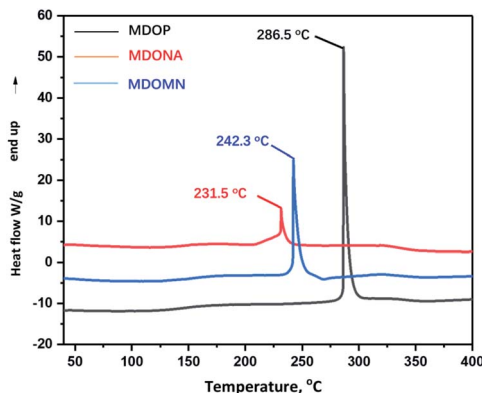


Fig. 6 DSC curves of MDONA, MDOMN, and MDOP.

detected by IR, the ion current at  $m/z = 28$  should be assigned to N<sub>2</sub>. Taking both IR and MS characterization into consideration, the gas products generated from thermal decomposition of MDO are primarily H<sub>2</sub>O, CO<sub>2</sub>, N<sub>2</sub>O, HCN, NH<sub>3</sub>, NO, NO<sub>2</sub>, and N<sub>2</sub>.

On the basis of the above-described DSC-TG-MS-IR analytical results and relative knowledge in the literature, we deduced a plausible thermal decomposition mechanism of MDO, as schematically illustrated in Scheme 4. Because of the strong polarity of N–O bond in MDO, the oxygen atom exhibits negative charge. This condition is very favorable for the transfer of proton from the adjacent amino group to oxygen atom. Hence, the oxygen atom is protonated to afford b.<sup>26</sup> With the increasing of temperature, b loses one molecule of water and decomposes

to c. Subsequently, the cleavage of C–N bond of c leads to the release of nitrogen oxides (e.g., N<sub>2</sub>O, NO, NO<sub>2</sub>). Meanwhile, owing to the instability of N=C=N bond, this bond of c cleaves and generates intermediate d. We inferred that the intermediate d may further decompose *via* two different pathways. The intermediate d might undergo coupling reaction to generate cross-linking compounds, or decompose into smaller molecules such as N<sub>2</sub> and NH<sub>3</sub>.<sup>27,28</sup>

### Thermal behaviours of MDOP, MDONA and MDOMN

Differential scanning calorimetric (DSC) and thermal gravimetric analyzer (TG) measurements were used to determine the thermo-dynamic stability of MDO energetic ionic salts from 40 °C to 400 °C. All these three energetic salts are decomposed directly without melting process. The decomposition temperatures ( $T_d$ ) of MDONA, MDOMN and MDOP are 231.5 °C, 242.3 °C and 286.5 °C, respectively (Fig. 6).

The decomposition temperatures of MDOMN and MDONA are obviously higher than that of RDX ( $T_d$ : 210 °C). It is noteworthy that MDOP exhibits good thermal stability that the decomposition temperature is 286.5 °C, which is significantly higher than RDX and even higher than HMX ( $T_d$ : 279 °C). In addition, MDONA, MDOMN and MDOP shows better thermal stability than the dianionic salts TTDON ( $T_d$ : 180 °C) and TTDOP ( $T_d$ : 176 °C).<sup>22</sup>

The DSC traces of MDONA, MDOMN and MDOP obtained at different heating rates of 2.5, 5, 10 and 20 °C min<sup>-1</sup> are shown in Fig. 7. Based on the Kissinger's and Ozawa-Doyle's methods, the non-isothermal kinetic parameters during the heating processes of MDONA, MDOMN and MDOP were investigated with the linear correlation coefficients ( $r$ ) of greater than 0.98. From Table 2, although the decomposition point of MDOP is the highest among these three compounds, the apparent activation energy  $E$  for it is the lowest of 116.16 kJ mol<sup>-1</sup> by Kissinger method and 165.78 kJ mol<sup>-1</sup> by Ozawa method.

### Physiochemical and energetic properties of MDO, MDOP, MDONA and MDOMN

The experimental density of MDO was 1.71 g cm<sup>-3</sup> as measured by gas pycnometer, which is comparable to the widely used insensitive reference thermostable explosive HNS ( $D$ : 1.70 g cm<sup>-3</sup>). Based on the heat of formation calculated by

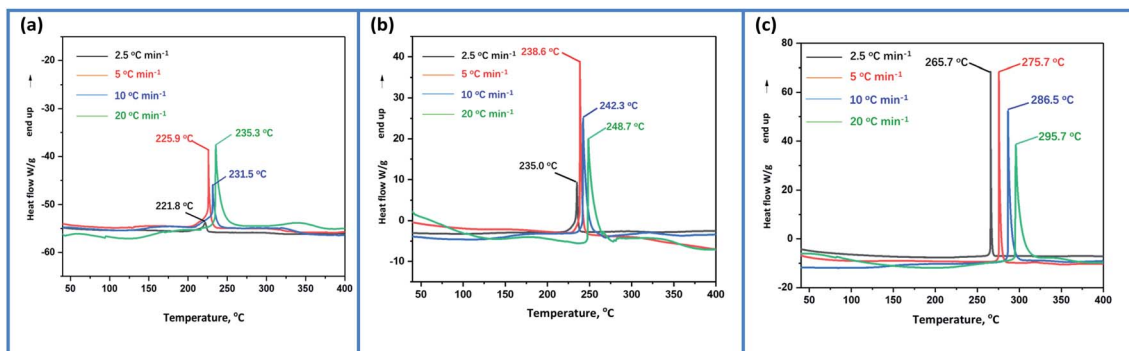


Fig. 7 DSC traces of MDONA (a), MDOMN (b) and MDOP (c) at different heating rates.



Table 2 Kinetic parameters and enthalpies of thermal decomposition of MDONA, MDOMN and MDOP

Comp.	$\beta$ (K min $^{-1}$ )	$T_p$ (K)	$E^a$ /(kJ mol $^{-1}$ )		$r^b$		$\ln(A_k^c$ s $^{-1}$ )
			Kissinger	Ozawa	Kissinger	Ozawa	
MDONA	2.5	494.98	306.69	298.11	0.99367	0.99441	73.56
	5	499.05					
	10	504.65					
	20	508.45					
MDOMN	2.5	508.15	329.46	321.45	0.98065	0.98162	77.10
	5	512.13					
	10	515.48					
	20	521.82					
MDOP	2.5	538.90	166.16	165.78	0.99818	0.99834	35.31
	5	548.82					
	10	559.65					
	20	568.82					

<sup>a</sup> Apparent activation energy. <sup>b</sup> Liner correlation coefficient. <sup>c</sup> Pre-exponential factor.

Table 3 Comparison of the physicochemical properties and detonation performances

Comp.	$T_d^a$ (°C)	$D^b$ (g cm $^{-3}$ )	$\Delta_fH^c$ (kJ mol $^{-1}$ )	$\Omega^d$ (%)	$v_D^e$ (m s $^{-1}$ )	$P^f$ (GPa)	IS $^g$ (J)	FS $^h$ (N)	$E_{50}^i$ (mJ)
MDO	319	1.71	-1.71	-70.9	6988	21.4	>40	>360	53
MDOP	287	1.89	104.4	-21.7	8711	34.4	23	240	97
MDONA	232	1.82	259.4	-21.1	9085	35.4	27	>360	153
MDOMN	242	1.75	59.5	-32.6	8857	32.3	27	>360	142
TTDON <sup>22</sup>	180	1.79	-31.5	-11.3	8900	34.2	14	—	—
TTDOP <sup>22</sup>	176	1.99	714.2	4.5	9284	41.0	13	—	—
HNS	315	1.70	78.2	-69.4	7000 (ref. 31)	21.8 (ref. 31)	5	240	62
RDX	210 (ref. 18)	1.80	86.3 (ref. 18)	-21.6	8795	34.9	7.5 (ref. 18)	120 (ref. 18)	70
HMX	279 (ref. 18)	1.90	116.1 (ref. 18)	-21.7	9144	39.2	7.51 (ref. 8)	120 (ref. 18)	37

<sup>a</sup> Decomposition temperature (exothermic peak). <sup>b</sup> Experimental density measured by gas pycnometer (25 °C). <sup>c</sup> Heats of formation calculated by Gaussian 09. <sup>d</sup> Oxygen balance (based on CO<sub>2</sub>) for C<sub>a</sub>H<sub>b</sub>O<sub>c</sub>N<sub>d</sub>, 16(c - (2a + 0.5b))/M<sub>w</sub>, M<sub>w</sub> = molecular weight. <sup>e</sup> Calculated detonation velocity (EXPLO5 v 6.01). <sup>f</sup> Calculated detonation pressure (EXPLO5 v 6.01). <sup>g</sup> Impact sensitivity evaluated by a standard BAM fall-Hammer. <sup>h</sup> Friction sensitivity evaluated by BAM technique. <sup>i</sup> Measured electrostatic-spark sensitivity,  $E_{50} = 1/2CV(50)^2$ .

Gaussian 09 program<sup>29</sup> and tested density, the detonation performances were calculated by EXPLO5 (v 6.01).<sup>30</sup> The results showed MDO possesses a detonation velocity of 6988 m s $^{-1}$  and a detonation pressure of 21.4 GPa, which are approximately equivalent to those of HNS. Furthermore, the tested impact sensitivity (IS) and friction sensitivity (FS) of MDO are greater than 40 J and 360 N, respectively. The electrostatic-spark sensitivity of MDO is 53 mJ, which is very close to that of HNS (Table 3).

In comparison with MDO, the ionic salts of MDO show higher densities and much improved detonation performances: the experimental densities of the energetic salts are between 1.75–1.89 g cm $^{-3}$ , the detonation velocities are greater than 8700 m s $^{-1}$ , which are similar to those of RDX. More importantly, these energetic salts also possess low sensitivities to impact (IS: >20 J), friction (FS: 240–360 N) and electrostatic-spark ( $E_{50}$ : >90 mJ). The sensitivity properties are apparently superior to those of RDX (IS: 7.4 J, FS: 120 J,  $E_{50}$ : 70 mJ) and HMX (IS: 7.4 J, FS: 120 J,  $E_{50}$ : 37 mJ). It's worth to point out that the reason of the thermal and mechanical stability of MDO are much better than that of MDOMN, MDOP and MDONA is

closely related to their molecular structure. From the crystal structure of MDO in Fig. S1,† MDO possesses a complete planar structure and all the atoms are in the same plane. Numerous strong intermolecular hydrogen bonds formed between the adjacent layers, which further afford MDO a face-to-face  $\pi$ - $\pi$  stacking structure and stabilized its solid structure. With the help of the  $\pi$ - $\pi$  stacking structure, the large conjugated system and large number of hydrogen bonds, MDO is insensitive to mechanical stimulation and has good thermal stability. After the introduction of anions (ClO<sub>4</sub> $^-$ , N(NO<sub>2</sub>)<sub>2</sub> $^-$  and NO<sub>3</sub> $^-$ ), the complete planar configuration was destroyed, so the thermal decomposition temperatures and mechanical stabilities of MDOP, MDOMN and MDONA decreased. Moreover, the oxygen content of the compounds increases significantly after the introduction of oxygen rich anions, and the increased O···O interactions will increase the mechanical sensitivity of the compounds. Compared with dianionic salts TTDON (IS: 14 J) and TTDOP (IS: 14 J),<sup>22</sup> the three energetic salts are less sensitivity to impact. These results clearly indicate that the energetic salts of MDO are a class of promising new energetic ionic salts with high energy and low sensitivity.



## Conclusions

In conclusion, we have demonstrated efficient synthetic and thermal studies on MDO based on oxidations of melamine structures. Thermal behavior of MDO in detail and possible thermal decomposition mechanism based on the results of TG-DSC-FTIR-MS technique were investigated for the first time. The gas products of MDO during the thermal decomposition are primarily  $\text{H}_2\text{O}$ ,  $\text{CO}_2$ ,  $\text{N}_2\text{O}$ ,  $\text{HCN}$ ,  $\text{NH}_3$ ,  $\text{NO}$ ,  $\text{NO}_2$ , and  $\text{N}_2$ . The apparent activation energy of MDO ( $E$ ) calculated by Kissinger and Ozawa method were 303.63 and 279.95  $\text{kJ mol}^{-1}$ , indicating the good thermal stability of MDO. Originated from the conjugated structure and the abundant hydrogen bonds between the amino group and  $N$ -oxide moiety, MDO exhibits similar performances to commonly used explosive HNS, representing a promising insensitive heat-resistant energetic compound. By tuning with energetic anions, three novel energetic ionic salts of MDO with improved performances, namely MDOP, MDONA, and MDOMN, were further designed and synthesized. MDOP, MDONA, and MDOMN possess thermal decomposition temperatures higher than 230 °C and decomposed directly without melting process. The three energetic salts hold satisfactory detonation performances ( $v_D$ : 8711–9085  $\text{m s}^{-1}$ ,  $P$ : 32.3–35.4 GPa) which are comparable to that of RDX, but with lower sensitivities to impact, friction and electrostatic-spark (IS: 23–27 J, FS: >240 J,  $E_{50}$ : 97–153 mJ), showing potential application prospect in the field of propellants.

## Conflicts of interest

There are no conflicts to declare.

## Acknowledgements

We are grateful to the financial support from National Natural Science Foundation of China (No. 21805223).

## Notes and references

- 1 C. J. Snyder, L. A. Wells, D. E. Chavez, G. H. Imler and D. A. Parrish, *Chem. Commun.*, 2019, **55**, 2461.
- 2 C. L. He, H. X. Gao, G. H. Imler, D. A. Parrish and J. M. Shreeve, *J. Mater. Chem. A*, 2018, **6**, 9391.
- 3 D. Fischer, T. M. Klapötke, D. G. Piercey and J. Stierstorfer, *Chem.-Eur. J.*, 2013, **19**, 4602.
- 4 Q. Wu, W. H. Zhu and H. M. Xiao, *RSC Adv.*, 2014, **4**, 53000.
- 5 A. A. Voronin, V. P. Zelenov, A. M. Churakov, Y. A. Strelenko and V. A. Tartakovskiy, *Russ. Chem. Bull.*, 2014, **63**, 475.
- 6 V. P. Zelenov, A. A. Voronin, A. M. Churakov, Y. A. Strelenko and V. A. Tartakovskiy, *Russ. Chem. Bull.*, 2014, **63**, 123.
- 7 A. M. Churakov, O. Y. Smirnov, S. L. Loffe, Y. A. Strelenko and V. A. Tartakovskiy, *Eur. J. Org. Chem.*, 2002, **14**, 2342.
- 8 Y. Shang, B. Jin, R. F. Peng, Z. C. Guo, Q. Q. Liu, J. Zhao and Q. C. Zhang, *RSC Adv.*, 2016, **6**, 48590.
- 9 H. Wei, H. Gao and J. M. Shreeve, *Chem.-Eur. J.*, 2015, **21**, 2726.

- 10 L. Hu, P. Yin, G. H. Imler, D. A. Parrish, H. X. Gao and J. M. Shreeve, *Chem. Commun.*, 2019, **55**, 8979.
- 11 M. S. Klenov, A. A. Guskov, O. V. Anikin, A. M. Churakov, Y. A. Strelenko, I. V. Fedyanin, K. A. Lyssenko and V. A. Tartakovskiy, *Angew. Chem., Int. Ed.*, 2016, **55**, 11472.
- 12 P. Politzer, P. Lane and J. S. Murray, *Cent. Eur. J. Energ. Mater.*, 2013, **10**, 37; K. O. Christe, D. A. Dixon, M. Vasiliu, R. I. Wagner, R. Haiges, J. A. Boatz and H. L. Ammon, *Propellants, Explos., Pyrotech.*, 2015, **40**, 463.
- 13 A. A. Voronin, V. P. Zelenov, A. M. Churakov, Y. A. Strelenko, I. V. Fedyanin and V. A. Tartakovskiy, *Tetrahedron*, 2014, **70**, 3018.
- 14 Y. F. Luo, F. Q. Bi, L. J. Zhai, X. Z. Li, J. L. Zhang and B. Z. Wang, *Chin. J. Energ. Mater.*, 2018, **26**, 919.
- 15 A. M. Churakov, S. L. Loffe and V. A. Tartakovskiy, *Mendeleev Commun.*, 1995, **5**, 227.
- 16 C. M. Tarver, P. A. Urtiew and T. D. Tran, *J. Energ. Mater.*, 2005, **23**, 183.
- 17 P. F. Pagoria, A. R. Mitchell and K. Bala, *US Pat.*, US20090299067 A1, 2009.
- 18 Y. Wang, Y. J. Liu, S. W. Song, Z. J. Yang, X. J. Qi, K. C. Wang, Y. Liu, Q. H. Zhang and Y. Tian, *Nat. Commun.*, 2018, **9**, 2444.
- 19 Y. X. Tang, C. L. He, G. H. Imler, D. A. Parrish and J. M. Shreeve, *ACS Appl. Energy Mater.*, 2019, **2**, 2263.
- 20 M. B. Talawar, R. Sivabalan, T. Mukundan, H. Muthurajan, A. K. Sikder, B. R. Gandhe and A. Subhananda Rao, *J. Hazard. Mater.*, 2009, **161**, 589.
- 21 J. R. Zhang, F. Q. Bi and B. Z. Wang, *50<sup>th</sup> International annual conference of the Fraunhofer ICT*, 2019, June 25–28.
- 22 S. W. Song, Y. Wang, W. He, K. C. Wang and Q. H. Zhang, *Chem. Eng. J.*, 2020, **35**, 125114.
- 23 H. E. Kissinger, *Anal. Chem.*, 1957, **29**, 1702.
- 24 T. A. Ozawa, *Bull. Chem. Soc. Jpn.*, 1965, **38**, 1881.
- 25 J. Zhou, L. Ding, F. Q. Zhao, B. Z. Wang and J. L. Zhang, *Chin. Chem. Lett.*, 2019, **31**, 554.
- 26 C. C. Ye, Q. An, T. Cheng, S. Zybinn, S. Naserifar, X. H. Ju and W. A. Goddard III, *J. Mater. Chem. A*, 2015, **3**, 12044.
- 27 G. Singh, I. P. Kapoor and S. K. Tiwari, *J. Hazard. Mater.*, 2001, **81**, 67.
- 28 I. P. Kapoor, P. Srivastava and G. Singh, *J. Hazard. Mater.*, 2008, **150**, 687.
- 29 M. J. Frisch, G. W. Trucks, H. B. Schlegel, G. E. Scuseria, M. A. Robb, J. R. Cheeseman, J. A. Montgomery Jr, T. Vreven, K. N. Kudin, J. C. Burant, J. M. Millam, S. S. Iyengar, J. Tomasi, V. Barone, B. Mennucci, M. Cossi, G. Scalmani, N. Rega, G. A. Petersson, H. Nakatsuji, M. Hada, M. Ehara, K. Toyota, R. Fukuda, J. Hasegawa, M. Ishida, T. Nakajima, Y. Honda, O. Kitao, H. Nakai, M. Klene, X. Li, J. E. Knox, H. P. Hratchian, J. B. Cross, V. Bakken, C. Adamo, J. Jaramillo, R. Gomperts, R. E. Stratmann, O. Yazyev, A. J. Austin, R. Cammi, C. Pomelli, J. W. Ochterski, P. Y. Ayala, K. Morokuma, G. A. Voth, P. Salvador, J. J. Dannenberg, V. G. Zakrzewski, S. Dapprich, A. D. Daniels, M. C. Strain, O. Farkas, D. K. Malick, A. D. Rabuck, K. Raghavachari, J. B. Foresman, J. V. Ortiz, Q. Cui, A. G. Baboul,



S. Clifford, J. Cioslowski, B. B. Stefanov, G. Liu, A. Liashenko, P. Piskorz, I. Komaromi, R. L. Martin, D. J. Fox, T. Keith, M. A. Al-Laham, C. Y. Peng, A. Nanayakkara, M. Challacombe, P. M. W. Gill, B. Johnson, W. Chen, M. W. Wong, C. Gonzalez and J. A. Pople, *Gaussian 09, rev. A.02*, Gaussian, Inc., Wallingford, CT, 2009.

30 M. Suceska, *EXPLO5, Version 6.04*, 2017.

31 B. Singh and R. K. Malhotra, *Def. Sci. J.*, 1983, **33**, 165.

